

DOI: 10.1070/QE2016v046n01ABEH015910

Superfocusing of an ultrashort plasmon pulse by a conducting cone

E.S. Manuilovich, V.A. Astapenko, P.A. Golovinskii

Abstract. **We have shown theoretically the possibility of controlling nanoscale superfocusing of plasmons in a metal conical tip by modulating the carrier frequency of the pulse. The propagation of an ultrashort plasmon pulse in a metal nanoneedle is simulated numerically. The calculation is based on an asymptotic analytical solution of Maxwell's equations for electromagnetic wave propagation in a conical conductor in the vicinity of its apex, obtained by the approximate separation of variables in spherical coordinates. The dependence the field superfocusing on the conductor material, pulse chirp and propagation length is studied.**

Keywords: *plasmon, ultrashort pulse, superfocusing, tip of a conducting cone.*

1. Introduction

Generation of femtosecond pulses of variable shape enables the control of complex quantum systems [1, 2]. To determine the general conditions for the optimal control of quantum-mechanical systems, Golovinskii [3] formulated a generalisation of Pontryagin's maximum principle. However, small sizes of nanostructures, as compared with the laser wavelength, complicate the spatial selectivity and independent control of individual nano-objects in such systems using laser light. Stockman et al. [4, 5] showed theoretically that limiting the localisation of the laser light impact by the diffraction limit can be overcome by the near-field effects of different nanoemitters. It was found that the spatial propagation of the near electromagnetic field can largely depend on the linear chirp (linear frequency modulation) of an incident laser pulse.

The combination of adaptive control [1, 2] and principles of nano-optics [6] allows subwavelength dynamic localisation of the field at nanoscale levels. If a conic conductor is used as a guiding structure, the propagation of a surface plasmon polariton along the conductor leads to a decrease in the wavelength as it approaches the apex of the cone. Babajanyan et al. [7] showed that as a result of this, the field is focused in a very small spatial region, whereas the electric field strength increases significantly. This phenomenon is used in the optical near-field microscopy for studying nanometre objects, because it provides a controlled 'delivery' of the field to them. Nonlocal effects arising due to the spatial dispersion result in a slight decrease in the field intensity [8, 9]. Numerical methods were used to study a reduction in the degree of maximal focusing due to the finite curvature of the tip [10] and the cone angle optimal for superfocusing was determined.

Theoretical works [11, 12] have shown the possibility of generating wave packets of plasmons (plasmon polaritons) in nanowires, which propagate along the nanoconductor and represent a superposition of plasmon modes in a multiresonance system. An interesting feature of the experimentally observed dynamics of these packets is the concentration of energy at the far or near end of the nanowires, or in its central portion, depending on the sign of the chirp or in its absence, respectively. The essence of the process is that the phase velocity of the lowest modes is higher than that of the highest modes, and a constructive interference arises between them at some distance from the excitation region. The field enhancement at the end of a silver nanowire was also observed experimentally [13, 14].

A unique feature of plasmon nanofocusing is the possibility of controlling the interference by adjusting spectral phases [15, 16]. A simultaneous use of spatial compression and femtosecond control of an optical excitation of surface plasmons in a conical metal nanotip can achieve a 10 nm spatially and few-femtosecond temporally confined excitation [17]. Thus, a possibility was demonstrated of spatial and temporal control of an optical field at nanometer scales and femtosecond durations. Experimentally, the femtosecond pulse propagation in a conical gold nanoprobe was observed in [18].

At the same time, details of the process of nanofocusing of ultrashort pulses are not yet entirely clear. Of interest are both the spatial focusing of the field near the tip and the concentration of the field in time. The aim of this paper is the numerical simulation of chirped ultrashort pulse amplification by conical metal structures, as well as analysis of the effect of the cone angle and the initial chirp of the pulse on the gain. The calculations were based on the results of paper [7] obtained for a monochromatic field. Using the inverse Fourier transform we have analysed the pulse propagation along a metal cone with characteristic cone angles of 0.01–0.1 rad, characteristic length of the order of several hundred nanometres at characteristic cone base size of less than 100 nm.

2. Field distribution under monochromatic excitation

The study of the dependence of the field enhancement near the cone tip on the polarisation of the exciting field for the transverse magnetic and linearly polarised waves which are

E.S. Manuilovich, V.A. Astapenko Moscow Institute of Physics and Technology (State University), Institutskii per. 9, 141707 Dolgoprudnyi, Moscow region, Russia;
e-mail: Egor.Manuylovich@gmail.com, astval@mail.ru;
P.A. Golovinskii Voronezh State University of Architecture and Civil Engineering, ul. 20-letiya Oktyabrya 84, 394030 Voronezh, Russia;
e-mail: golovinski@bk.ru

Received 27 July 2015; revision received 23 November 2015
Kvantovaya Elektronika **46** (1) 50–56 (2016)
Translated by I.A. Ulitkin

focused on the base of the cone showed that the effective field enhancement is typical of a symmetric TM ($m = 0$) wave [19]. This type of polarisation can be obtained, for example, by direct focusing of radially polarised laser beams in nanocones [20]. In this regard, we will confine our consideration below to a wave packet of TM_0 waves.

The main difference of this problem from the classical problem of diffraction theory [21] is that the traditional assumption about the surface character of the skin effect cannot be satisfied, and it is necessary to use real experimental frequency dependences of complex dielectric constants of metals [22] or their convenient analytical approximations [23, 24]. The analytical solution of the problem of propagation and superfocusing of a harmonic surface plasmon in a narrow metal cone that is used in the analysis of our problem is given by Babajanyan et al. [7], who considered an interesting for us magnetic type of transverse waves, for which only the vortex component $H_\varphi \neq 0$. The geometry of the problem is shown in Fig. 1.

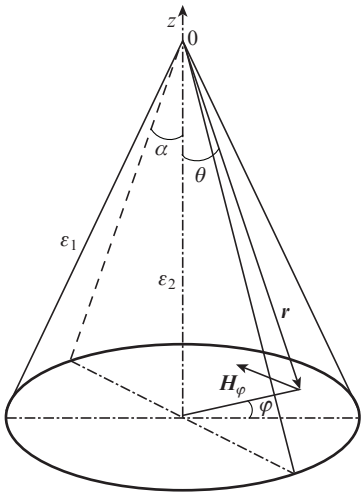

Figure 1. Geometry of a conical structure in which superfocusing is performed; ε_1 and ε_2 are the dielectric constants outside and inside the cone, respectively.

For further analysis, we expound, first, closely following [7], the solution of the problem of propagation of monochromatic waves. For the H_φ component the propagation equation is transformed into a scalar equation. In spherical coordinates we can write it in the form of the wave equation [25]

$$\frac{1}{r}\frac{\partial^2}{\partial r^2}(rH_\varphi) + \frac{1}{r^2}\frac{\partial}{\partial\theta}\left[\frac{1}{\sin\theta}\frac{\partial(H_\varphi\sin\theta)}{\partial\theta}\right] = \frac{\varepsilon}{c^2}\frac{\partial^2 H_\varphi}{\partial t^2}, \qquad (1)$$

where $\varepsilon(\omega)$ is the dielectric constant of the medium (the permeability $\mu = 1$); ω is the frequency of the wave; and c is the speed of light. For separation of the variables we represent solution (1) in the form

$$H_\varphi(r,\theta,t) = R(r)\Psi(\theta)\exp(-i\omega t). \qquad (2)$$

Then for the functions $\Psi(\theta)$ and $R(r)$ we obtain the equations:

$$\frac{d^2\Psi}{d\theta^2} + \frac{\cos\theta}{\sin\theta}\frac{d\Psi}{d\theta} - \left(\eta^2 + \frac{1}{\sin^2\theta}\right)\Psi = 0, \qquad (3)$$

$$\frac{d^2R}{dr^2} + \frac{2}{r}\frac{dR}{dr} - \left(\frac{\eta^2}{r^2} + \varepsilon\frac{\omega^2}{c^2}\right)R = 0, \qquad (4)$$

in which the constant of separation of variables η is determined from the boundary conditions on the surface of the cone. For small cone angles α, the parameter $\theta \ll 1$ rad, both inside and outside the cone, is near its surface. Accordingly, equation (3) without significant loss of accuracy can be replaced by the equation

$$\frac{d^2\Psi}{d\theta^2} + \frac{1}{\theta}\frac{d\Psi}{d\theta} - \left(\eta^2 + \frac{1}{\theta^2}\right)\Psi = 0, \qquad (5)$$

which after the replacement of variables $x = \eta\theta$ takes the form

$$x^2\frac{d^2\Psi}{dx^2} + x\frac{d\Psi}{d\theta} - (x^2+1)\Psi = 0. \qquad (6)$$

The solution to equation (6) at $x \geqslant 0$ is expressed via the modified Bessel function $I_1(x)$ and the Macdonald function $K_1(x)$ [26]:

$$\Psi(x) = D_1 I_1(x) + D_2 K_1(x). \qquad (7)$$

In this case, the function $I_1(x)$ is regular at zero, and the function $K_1(x)$ falls off exponentially at large x. Therefore, the solution to equation (3) for two different ranges of angles has the form

$$\Psi(\theta) = D_1 I_1(\eta\theta), \quad \theta \leqslant \alpha, \qquad (8)$$

$$\Psi(\theta) = D_2 K_1(\eta\theta), \quad \theta \geqslant \alpha. \qquad (9)$$

We note that the smallness of the cone angle allows one to obtain and investigate analytically the solution. Similarly, it is possible to solve the problem of the conical cavity [27]. The equation for the radial function (4) is analogous to the equation for the radial function in the quantum-mechanical problem of motion in a centrally symmetric field of the polarisation potential [28]. We introduce the notation $W = \varepsilon\omega^2/c^2$ and make the replacement $R(r) = \chi(r)/r$. For the new function $\chi(r)$, instead of (4), we have the equation

$$\chi'' + \left(\frac{\eta^2}{r^2} + W\right)\chi = 0.$$

If we now make the substitution

$$\chi(r) = \sqrt{r}\,Z(\rho), \quad \rho = kr,$$

where $k = \sqrt{W}$, we obtain the equation

$$\rho^2 Z'' + \rho Z' + (\rho^2 + \nu^2) = 0, \quad \nu^2 = \eta^2 - 1/4. \qquad (10)$$

At $\eta^2 > 1/4$, equation (10) is a differential equation for the Bessel functions with a pure imaginary index [29], the solutions of which are sufficiently studied. The equation has two independent solutions – $Sf_\nu(x)$ and $Cf_\nu(x)$, which are expressed in the form of absolutely convergent series at any values of x and ν:

$$Sf_\nu(x) = \left[1 - \frac{1}{1+\nu^2}\left(\frac{x}{2}\right)^2 + \ldots\right]\times$$

$$\times\sin(v\ln x)+\left[\frac{v}{1+v^2}\left(\frac{x}{2}\right)^2+\ldots\right]\cos(v\ln x), \tag{11}$$

$$\mathrm{Cf}_v(x)=\left[1-\frac{1}{1+v^2}\left(\frac{x}{2}\right)^2+\ldots\right]$$

$$\times\cos(v\ln x)+\left[\frac{v}{1+v^2}\left(\frac{x}{2}\right)^2+\ldots\right]\sin(v\ln x). \tag{12}$$

At the values of the argument $x \to 0$ we have asymptotic representations $\mathrm{Sf}_v(x) \propto \sin(v\ln x)$, $\mathrm{Cf}_v(x) \propto \cos(v\ln x)$.

Given this near the cone apex at $\eta^2/r^2 \gg |\varepsilon|\omega^2/c^2$, valid is the asymptotic expression

$$H_\varphi \approx \frac{A(\omega)}{\sqrt{r}}\Psi(\theta)\exp\left(-\mathrm{i}\omega t-\mathrm{i}v\ln\frac{r}{r_0}\right), \tag{13}$$

where the distance r_0 from the section to the cone apex determines the phase of the wave. On the basis of Maxwell's equations we obtain

$$E_r=\frac{\mathrm{i}c}{\omega\varepsilon}\frac{1}{r\sin\theta}\frac{\partial(H_\varphi\sin\theta)}{\partial\theta}, \tag{14}$$

$$E_\theta=-\frac{\mathrm{i}c}{\omega\varepsilon}\frac{\partial}{\partial r}(rH_\varphi). \tag{15}$$

Then the spatial dependences of the electrical components of the monochromatic field have the form

$$E_r(\omega)=-\frac{\mathrm{i}c}{\omega\varepsilon_2}\frac{\eta A(\omega)}{r^{3/2}}I_0(\eta\theta)\exp\left(-\mathrm{i}\eta\ln\frac{r}{r_0}\right), \tag{16}$$

$$E_\theta(\omega)=\frac{\mathrm{i}c}{\omega\varepsilon_2}\left(\eta+\frac{\mathrm{i}}{2}\right)\frac{A(\omega)}{r^{3/2}}I_1(\eta\theta)\exp\left(-\mathrm{i}\eta\ln\frac{r}{r_0}\right) \tag{17}$$

at $\theta \leqslant \alpha$ and

$$E_r(\omega)=\frac{\mathrm{i}c}{\omega\varepsilon_1}\frac{\eta B(\omega)}{r^{3/2}}K_0(\eta\theta)\exp\left(-\mathrm{i}\eta\ln\frac{r}{r_0}\right), \tag{18}$$

$$E_\theta(\omega)=\frac{\mathrm{i}c}{\omega\varepsilon_1}\left(\eta+\frac{\mathrm{i}}{2}\right)\frac{B(\omega)}{r^{3/2}}K_1(\eta\theta)\exp\left(-\mathrm{i}\eta\ln\frac{r}{r_0}\right) \tag{19}$$

at $\theta \geqslant \alpha$. Here, I_0 and K_0 are the modified Bessel function and the zero-order Macdonald function, respectively. These solutions predict a singular growth of the wave field near the apex of the cone, limited by the length of the upper base of the truncated cone to its geometric apex.

3. Focusing of an ultrashort plasmon-polariton pulse

To solve the problem of spatiotemporal focusing, we assume that in the case of an incident ultrashort laser pulse exciting a magnetic-type wave in a conical structure, the time dependence of the electric field in the centre of the cross section at a distance h from the top has the form $f(t) = C(t)\exp[-\mathrm{i}\omega_0 t - \mathrm{i}\psi(t)]$, where $\psi(t) = \omega_0\beta t^2$, i.e. the effective frequency has a linear chirp β: $\omega_{\mathrm{eff}}(t) = \omega_0(1 + \beta t)$. For a Gaussian pulse $C(t) = f_0\exp(-at^2)$, and the corresponding intensity is $I(t) = f(t)f^*(t) = f_0^2\exp(-2at^2)$. The Fourier transform of this pulse [30] is

$$\tilde{f}(\omega)=\frac{1}{2\pi}\int_{-\infty}^{\infty}f(t)\exp(-\mathrm{i}\omega t)\,\mathrm{d}t$$

$$=\frac{f_0}{\sqrt{4\pi(a+\mathrm{i}\beta)}}\exp\left[-\frac{(\omega-\omega_0)^2}{4(a+\mathrm{i}\beta)}\right]. \tag{20}$$

The evolution of the pulse in the linear regime is completely determined by the inverse Fourier transform:

$$E_j(r,\theta,t)=\int_{-\infty}^{\infty}\tilde{f}(\omega)\,E_j(\omega)\exp(\mathrm{i}\omega t)\,\mathrm{d}\omega,\quad j=r,\theta. \tag{21}$$

To calculate the Fourier integral (21) we need to know the dependence of the parameter $\eta = \eta' + \mathrm{i}\eta''$ on the frequency ω. This dispersion dependence is determined from the condition of continuity of the tangential components of the field on the surface of the cone. The corresponding dispersion equation has the form

$$\varepsilon_2\frac{I_1(\alpha\eta)}{I_0(\alpha\eta)}=-\varepsilon_1\frac{K_1(\alpha\eta)}{K_0(\alpha\eta)}, \tag{22}$$

where $\varepsilon_2 = \varepsilon_2' + \mathrm{i}\varepsilon_2''$. By specifying $E_r(h,t) = f(t)$, we find $A(\omega)$ and the spectral components $E_r(r,\omega)$, $E_\theta(r,\omega)$ inside the cone, and from the condition of matching solutions on the boundary of the cone we determine the value of $B(\omega)$ and spectral components of the field outside the cone. Parameters A and B are measured in V m$^{-1/2}$.

The values of real and imaginary parts of the refractive index are taken from [31]. We used them to calculate real and imaginary parts of the dielectric constant of metals. Then, we numerically solved equation (22) for each spectral component. The results of calculations of the dependences of real and imaginary parts of the propagation parameter η on the wavelength λ are shown in Fig. 2 for silver, gold and copper nanoneedles in vacuum. Using the results of calculations of the propagation parameter η' we can estimate the effective refractive index in the medium, as well as the phase and group velocities of the packet. Figure 3 shows the dependence of the effective refractive index $n_{\mathrm{eff}} = n'_{\mathrm{eff}} + \mathrm{i}n''_{\mathrm{eff}}$ in a silver cone with an opening angle $\alpha = 0.01$ rad on the distance z to the apex of the cone. One can clearly see its increase with approaching to the apex.

Figure 4 shows the dependence of the phase and group velocities on z for the same cone. At a distance of 500 m from the apex at the centre wavelength $\lambda_0 = 1550$ nm the group velocity is equal to $0.18c$; with a further approach to the apex of the cone the wave virtually stops.

For each spectral component we calculated the change in the flow of energy as it propagates to the cone apex. The energy flow was calculated by the formula

$$F=\int_S[E_r(\omega,r,\theta)E_r^*(\omega,r,\theta)$$

$$+E_\theta(\omega,r,\theta)E_\theta^*(\omega,r,\theta)]v_{\mathrm{p}}(\omega)\,\mathrm{d}S, \tag{23}$$

where S is the cone section plane perpendicular to its generatrix, and $v_{\mathrm{p}}(\omega)$ is the phase velocity of the spectral component. Figure 5 shows the attenuation of the flow of the spectral components after their propagation from a distance of 1000 nm up to a distance of 100 nm from the apex of a silver cone. Despite the fact that the energy flow of each spectral component is significantly attenuated as it propagates along the cone due to absorption in the metal, the electromagnetic

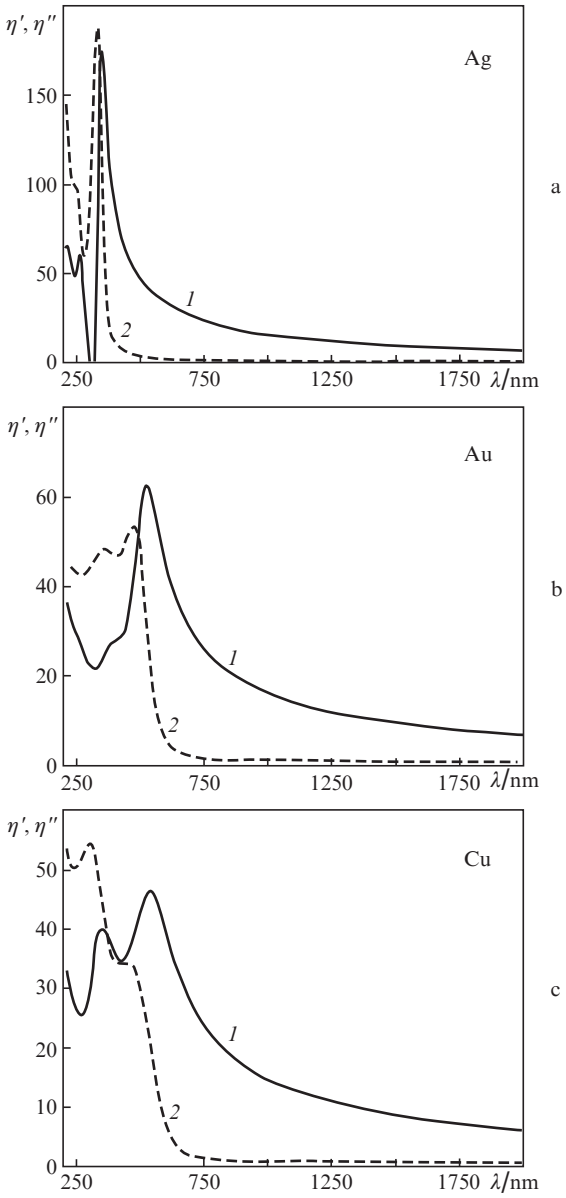

Figure 2. Dependences of (*1*) real and (*2*) imaginary parts of the propagation constant η on the laser wavelength λ for (a) silver, (b) gold and (c) copper nanoneedles with a cone angle 0.01 rad.

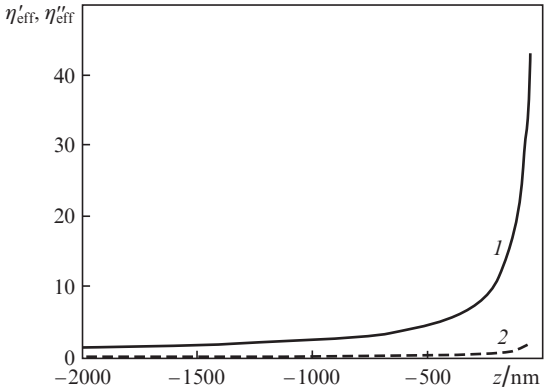

Figure 3. Dependences of (*1*) real and (*2*) imaginary parts of the effective refractive index on the distance to the apex of the cone at the centre wavelength $\lambda_0 = 1550$ nm.

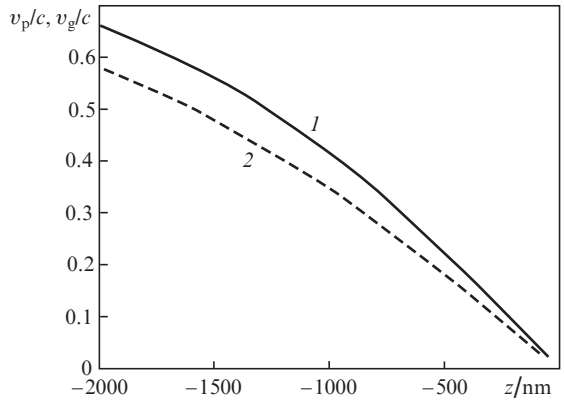

Figure 4. Dependences of (v_p; *1*) phase and (v_g; *2*) group velocities on the distance z to the apex of the cone at the wavelength $\lambda_0 = 1550$ nm.

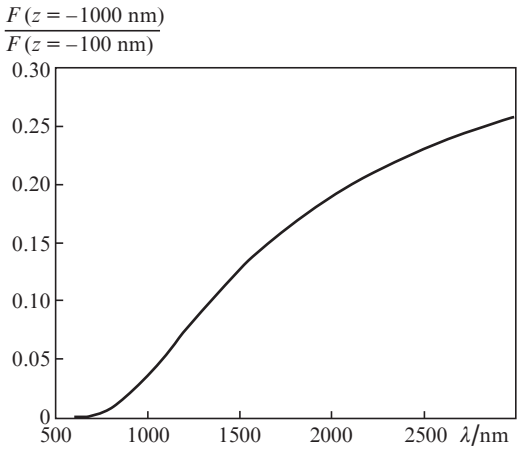

Figure 5. Dependence of the energy flow attenuation on the laser wavelength.

field of the spectral components increases as it approaches the apex of the cone due to the increase in the spatial localisation of the field.

Figures 6–8 show the results of calculation of the field on the surface of silver, gold and copper nanoneedles for a 32-fs chirpless and positively (negatively) chirped laser pulse with a centre wavelength of 1550 nm. The angle of the cone for all calculations was 0.01 rad. The pulse travels a distance from 1000 nm to 100 nm from the apex of a metal cone.

For Figs 6a, 6b and 6c the gain in a silver cone is 11.62, 11.44 and 13.69, and the change in the pulse duration is equal to 0.2, 5.3 and –6.4 fs, respectively. For Figs 7a, 7b and 7c the gain in a gold cone is 7.28, 7.02 and 10.15, and the change in the pulse duration is equal to 0.2, 6.1 and –6.4 fs, respectively. For Figs 8a, 8b and 8c the gain in a copper cone is 6.23, 6.05 and 7.57, and the change in the pulse duration is equal to 0, 4.9 and –4.6 fs, respectively.

For the silver cone we calculated the gain (at the same parameters as before) as a function of the cone angle for a laser pulse without an initial chirp, with a centre wavelength of 1550 nm and an initial duration of 32 fs. The results of calculations are presented in Fig. 9. It can be seen that by increasing the cone angle the focusing effect is enhanced. In fact, at $\alpha \approx 14°$, this enhancement is already close to the maximal. It should be noted that a further increase in the angle actually does not guarantee the growth of the focused field,

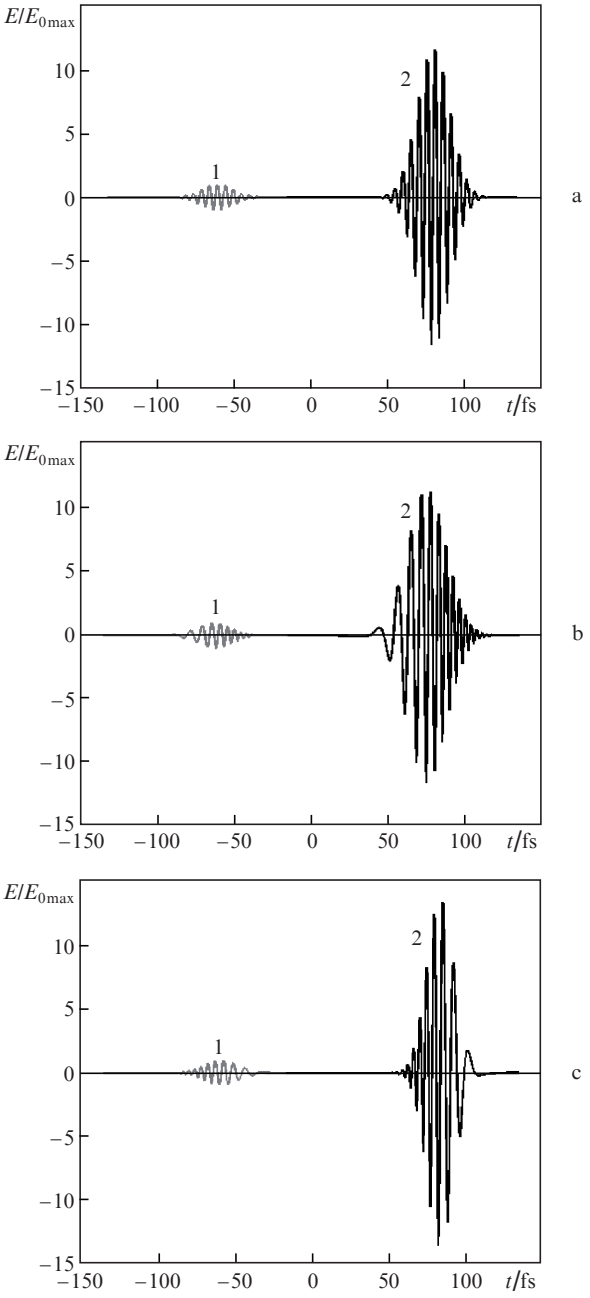

Figure 6. Results of calculation of the electric field E to the pulse (1) before and (2) after its propagation in a silver cone for initial chirps of the pulse β = (a) 0, (b) −0.013 and (c) 0.013 fs^{-1}.

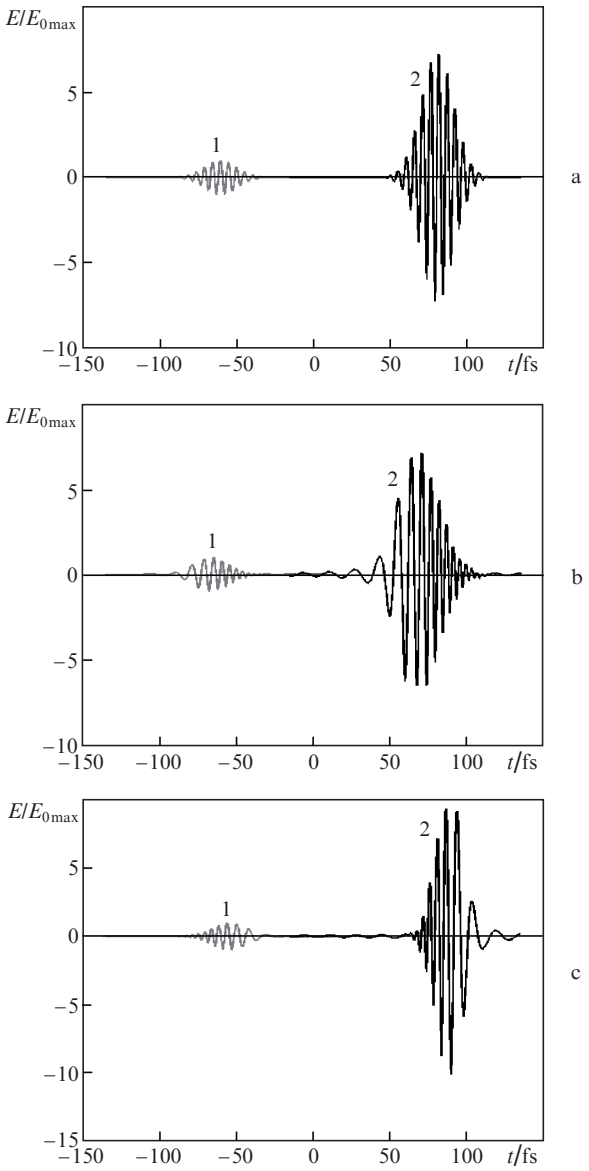

Figure 7. Same as in Fig. 6, but during the propagation of a pulse in a gold cone.

because the field is transferred to other modes due to the violation of single-mode propagation [32].

For the silver cone we also calculated the gain and compression ratio of the pulse as a function of its initial chirp. The calculation was performed, starting with the distance of 1000 nm to 150 nm from the apex of the cone with an opening angle of $\alpha = 0.1$ rad. The calculation results are shown in Fig. 10 for the initial pulse duration $\tau_0 = 32$ fs and the centre wavelength $\lambda_0 = 1550$ nm. It follows from Fig. 10 that the change in the initial chirp of pulse allows one to reach a 10% enhancement of the focusing effect with respect to the gain and a 10% pulse compression. Our results are consistent with the overall picture of spatiotemporal superfocusing observed in the experiment [17].

4. Conclusions

Analytical formulas for the field near the apex of a metal cone have allowed us to calculate the propagation of ultrashort plasmon pulses in nanoneedles of three metals: silver, gold and copper. We have calculated the propagation constant as a function of frequency and determined the phase and group velocities of propagation as functions of the distance to the apex of the cone. When approaching to the apex of the cone the velocity of the pulse is reduced, and the field of the electromagnetic wave is amplified. Superfocusing of plasmon pulses is observed in a metal cone and the gain depends on the material of the cone. When the pulse travels a distance of 850 nm in a conical structure of length 1000 nm at an opening angle $\alpha = 0.01$ rad, we have observed that the electric field of a 32-fs nonchirped pulse increases by 11.6 times for the silver cone, by 7.3 times for the golden cone and by 6.2 times for the copper cone. A further enhancement of the focusing effect can be achieved at a greater angle of the cone.

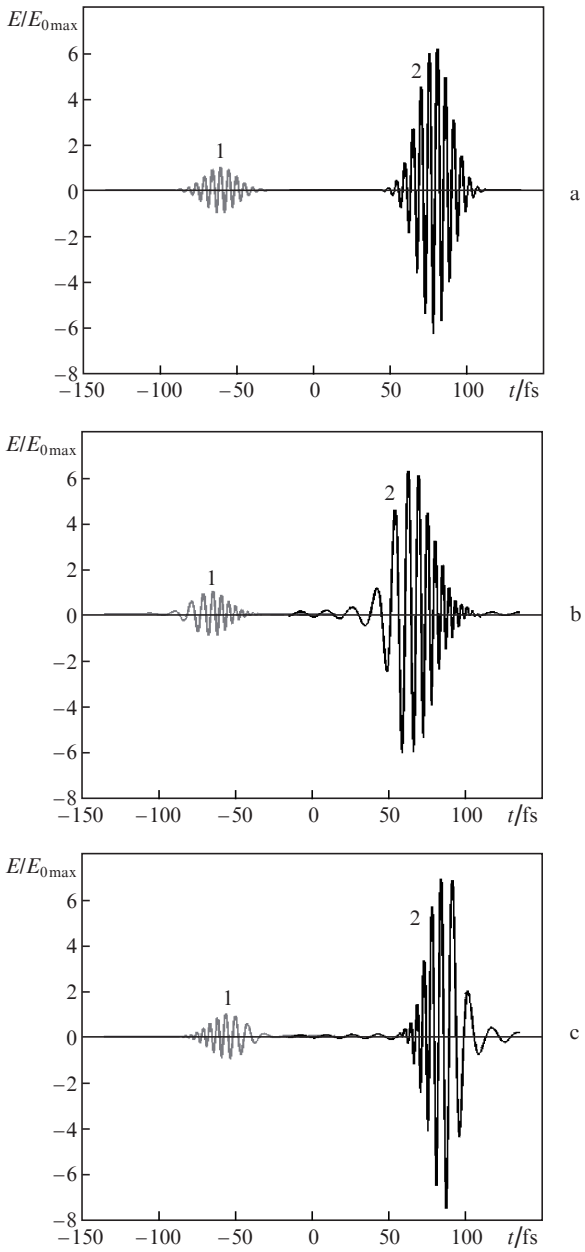

Figure 8. Same as in Fig. 6, but during the propagation of a pulse in a copper cone.

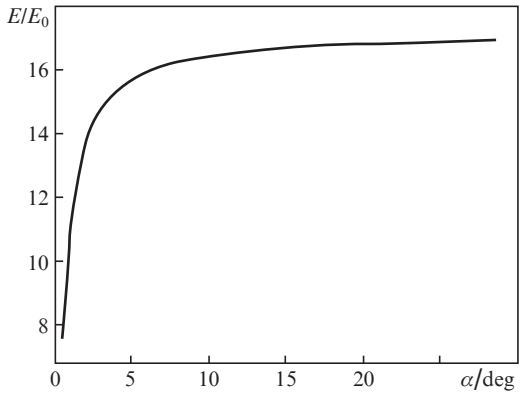

Figure 9. Dependence of the pulse gain E/E_0 on the opening angle of the silver cone.

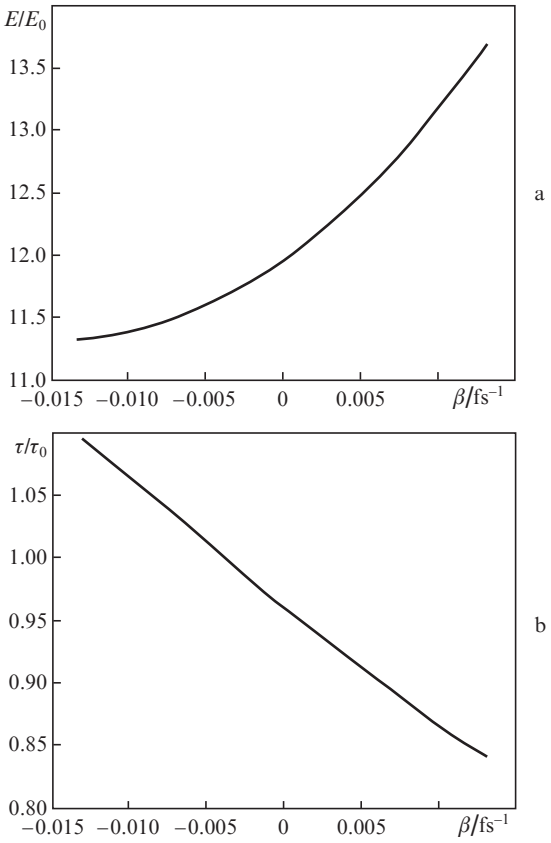

Figure 10. Dependences of (a) the gain E/E_0 and (b) pulse duration τ/τ_0 on the initial chirp β.

The focusing effect is enhanced in the case of pulses with a negative initial chirp. This allows the use of frequency modulation to obtain optimal superfocusing of a femtosecond plasmon pulse.

Acknowledgements. This work was supported by the Russian Foundation for Basic Research (Grant No. 15-07-09123) and performed within the framework of the State Task of the RF Ministry of Education and Science (Research No. 1940).

References

1. Judson R.S., Rabitz H. *Phys. Rev. Lett*., **68**, 1500 (1992).
2. Assion A., Baumert T., Bergt M., Brixner T., Kiefer B., Seyfried V., Strehle M., Gerber G. *Science*, **282**, 919 (1998).
3. Golovinskii P.A. *Avtomat. Telemekh*., **4**, 42 (2007).
4. Stockman M.I., Faleev S.V., Bergman D.J. *Phys. Rev. Lett*., **88**, 067402 (2002).
5. Stockman M.I., Bergman D.J., Kobayashi T. *Phys. Rev. B*, **69**, 054202 (2004).
6. Novotny L., Hecht B. *Principles of Nano-Optics* (Cambridge: Cambridge University Press, 2006).
7. Babajanyan A.J., Margaryan N.L., Nerkararyan Kh.V. *J. Appl. Phys*., **87**, 3785 (2000).
8. Ruppin R. *Phys. Lett. A*, **340**, 299 (2005).
9. Wiener A., Fernández-Domínguez A.I., Horsfield A.P., Pendy J.B. *Nano Lett*., **12**, 3308 (2012).
10. Goncharenko A.V., Wong J.K., Chang Y.-Ch. *Phys. Rev. B*, **74**, 235442(9) (2006).
11. Aeschlimann M., Bauer M., Bayer D., Brixner T., de Abajo F.J.G., Pfeiffer W., Rohmer M., Spindler C., Steeb F. *Nature*, **446**, 310 (2007).
12. Cao L., Nome R.A., Montgomery J.M., Gray S.K., Scherer N.F. *Nano Lett*., **10** (9), 3389 (2010).

13. Ditlbacher H., Honenan A., Wagner D., Aussenegg F.R., Krenn J.R. *Phys. Rev. Lett*., **95**, 257403(4) (2005).
14. Li Z., Hao F., Huang Y., Fang Y., Nordlander P., Xu H. *Nano Lett*., **9** (12), 4383 (2009).
15. Berweger S., Atkin J.M., Olmon R.L., Rashke M.B. *J. Phys. Chem. Lett*., **3**, 9450952 (2012).
16. Stockman M.I., Faleev S.V., Bergman D.J. *Phys. Rev. Lett*., **88** (6), 067402(4) (2002).
17. Berweger S., Atkin J.M., Xu X.G., Olmon R.L., Rashke M.B. *Nano Lett*., **11**, 4309 (2011).
18. Kravtsov V., Atkin J.M., Rashke M.B. *Opt. Lett*., **38**, 1322 (2013).
19. De Angelis F., Proietti Zaccaria R., Francardi M., Liberale C., Di Fabrizio E. *Opt. Express*, **19** (22), 22268 (2011).
20. Agio M., Chen X.W., Sandonghdar V. *Opt. Express*, **18** (10), 10878 (2010).
21. Vaganov R.B., Katsenelenbaum B.Z. *Osnovy teorii difraktsii* (Foundations of Diffraction Theory) (Moscow: Nauka, 1982).
22. Jonson P.B., Christy R.W. *Phys. Rev. B*, **6**, 4370 (1972).
23. Dionne J.A., Sweatlock L.A., Atwater H.A. *Phys. Rev. B*, **72**, 075405 (2005).
24. Barchiesi D., Grosges T. *J. Nanophotonics*, **8**, 083097(16) (2014).
25. Koshlyakov N.S., Gliner E.B., Smirnov M.M. *Basic Differential Equations of Mathematical Physics* (Amsterdam: North-Holland; New York: Wiley, 1964; Moscow: GIFML, 1962).
26. Nikiforov A.F., Uvarov V.B. *Special Functions of Mathematical Physics. A Unified Introduction with Applications* (Basel: Birkhäuser Verlag, 1988; Dolgoprudnyi: Intellect, 2007).
27. Alekseenko Ya.V., Monakhov A.M., Rozhanskii I.V. *Zh. Tekh. Fiz*., **79** (11), 72 (2009).
28. Landau L.D., Lifshitz E.M. *Quantum Mechanics. Non-relativistic Theory* (Oxford, New York: Pergamon Press, 1977; Moscow: Fizmatlit, 2008).
29. Matushev A.A., Fohtung E.B. *Nauchn. Priborostr*., **26** (1), 144 (2014).
30. Gradshteyn I.S., Ryzhik I.M. *Tables of Integrals, Series and Products* (Boston: Acad. Press, 1994; St. Petersburg: BKhV–Petersburg, 2011).
31. Rakić A.D., Djurišic A.B., Elazar J.M., Majewski M.L. *Appl. Opt*., **37**, 5271 (1998).
32. Ding W., Andrews S.R., Mailer S.A. *Phys. Rev. A*, **75**, 063822(10) (2007).